

U.S. DEPARTMENT OF COMMERCE
National Technical Information Service

AD-A024 591

ADDITIONAL ENERGY SOLUTIONS FOR PREDICTING
STRUCTURAL DEFORMATIONS

SOUTHWEST RESEARCH INSTITUTE

PREPARED FOR
EDGEWOOD ARSENAL

NOVEMBER 1975

145100

AD

EDGEWOOD ARSENAL CONTRACTOR REPORT
EM-CR-76031
Report No. 4

AD A 024591

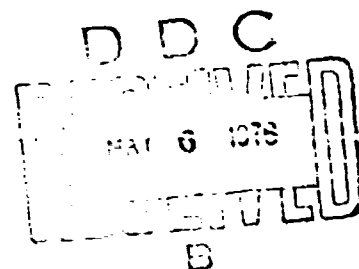
ADDITIONAL ENERGY SOLUTIONS FOR
PREDICTING STRUCTURAL DEFORMATIONS

by

P. S. Westine

P. A. Cox

November 1975



SOUTHWEST RESEARCH INSTITUTE
Post Office Drawer 28510, 8500 Culebra Road
San Antonio, Texas 78284

Contract No. DAAA15-75-C-0083



DEPARTMENT OF THE ARMY
Headquarters, Edgewood Arsenal
Aberdeen Proving Ground, Maryland 21010



Approved for public release; distribution unlimited

REPRODUCED BY
NATIONAL TECHNICAL
INFORMATION SERVICE
U. S. DEPARTMENT OF COMMERCE
SPRINGFIELD, VA 22161

UNCLASSIFIED

SECURITY CLASSIFICATION OF THIS PAGE (When Data Entered)

REPORT DOCUMENTATION PAGE		READ INSTRUCTIONS BEFORE COMPLETING FORM
1. REPORT NUMBER EM-CR-76031	2. GOVT ACCESSION NO.	3. RECIPIENT'S CATALOG NUMBER
4. TITLE (and Subtitle) ADDITIONAL ENERGY SOLUTIONS FOR PREDICTING STRUCTURAL DEFORMATIONS		5. TYPE OF REPORT & PERIOD COVERED Technical Report Sept. 1974 to July 1975
		6. PERFORMING ORG REPORT NUMBER Report No. 4
7. AUTHOR(s) P. S. Westine P. A. Cox		8. CONTRACT OR GRANT NUMBER(s) DAAA15-75-C-0083
9. PERFORMING ORGANIZATION NAME AND ADDRESSES Southwest Research Institute P. O. Drawer 28510 San Antonio, Texas 78284		10. PROGRAM ELEMENT, PROJECT, TASK AREA & WORK UNIT NUMBERS PA, A 5751264
11. CONTROLLING OFFICE NAME AND ADDRESS Commander, Edgewood Arsenal Attn: SAREA-TS-R Aberdeen Proving Ground, Maryland 21010		12. REPORT DATE November 1975
		13. NUMBER OF PAGES 34
14. MONITORING AGENCY NAME & ADDRESS (if different from Controlling Office) Commander, Edgewood Arsenal Attn: SAREA-MT-H Aberdeen Proving Ground, MD 21010 (CPO Mr. Bruce Jezek, 671-2661)		15. SECURITY CLASS (of this report) UNCLASSIFIED
		15a. DECLASSIFICATION DOWNGRADING SCHEDULE NA
16. DISTRIBUTION STATEMENT (of this Report) Approved for public release; distribution unlimited.		
17. DISTRIBUTION STATEMENT (of the abstract entered in Block 20, if different from Report)		
18. SUPPLEMENTARY NOTES		
19. KEY WORDS (Continue on reverse side if necessary and identify by block number) Energy solutions Impulsive response Quasi-static response Beams Plates Shells Plastic deformation		
20. ABSTRACT (Continue on reverse side if necessary and identify by block number) Revised and newly developed formulas for prediction of plastic deformations of structural elements in suppressive structures are presented in this report. These equations give improved agreement with literature, data and solutions for more structural elements than previous reports.		

DD FORM 1473
1 JAN 73

EDITION OF 1 NOV 55 IS OBSOLETE

UNCLASSIFIED

SECURITY CLASSIFICATION OF THIS PAGE (When Data Entered)

SUMMARY

Revised and newly developed formulas for prediction of plastic deformations of structural elements in suppressive structures are presented in this report. These formulas supplement previously reported design equations. Revised equations give improved agreement with literature data, while equations for additional structural elements allow prediction for a wider spectrum of structural components. Some comparisons are made of predictions from these design formulas with results of computer code calculations.

PREFACE

The investigation described in this report was authorized under PA, A 4932, Project 5751264. The work was performed at Southwest Research Institute under Contract DAAA15-75-C-0083.

The use of trade names in this report does not constitute an official endorsement or approval of the use of such commercial hardware or software. This report may not be cited for the purposes of advertisement.

The information in this document has been cleared for release to the general public.

TABLE OF CONTENTS

	<u>Page</u>
LIST OF ILLUSTRATIONS	6
I. INTRODUCTION	7
II. ANALYSIS	7
A. General	7
B. Clamped Circular Plates	8
C. Clamped Rectangular Plates	12
D. Rings Constraining I-beams	21
E. Hemispheres (Domes)	25
III. RESULTS	28
IV. DISCUSSION	29
REFERENCES	33

LIST OF ILLUSTRATIONS

<u>Figure</u>		<u>Page</u>
1	Plate Deformations in an Impulsed Clamped Circular Plate	10
2	Measured Loading in NSRDC Circular Plate Tests	12
3	Deformation in Quasi-Statically Loaded Circular Plate	13
4	Predicted and Experimental Deformations in Uniformly Impulsed Rectangular Plates	17
5	Permanent Deformations in Quasi-Statically Loaded Square Plate	19
6	Permanent Deformations in Quasi-Statically Loaded Rectangular Plate	20
7	Geometry of Beams and Rings in the Cylinder Wall	22
8	Schematic of Error Incurred by Assumption of Constant Quasi-Static Pressure, P	23
9	Symmetry of Dome Geometry, Loading and Response	25
10	Geometry of the Double-Dome Separated by Filler Material	28

ADDITIONAL ENERGY SOLUTIONS FOR PREDICTING STRUCTURAL DEFORMATIONS

I. INTRODUCTION

A number of structural design equations have been developed in the suppressive structures program to predict the plastic deformations of various structural elements to blast loads. These equations are based on the principles of limit design which allow large plastic deformation short of collapse or failure, and on energy balance principles. References 1 and 2 report our initial efforts in development of such structural response equations, and include design formulas for predicting permanent deformations of simple rigid-plastic systems, beams with various boundary conditions, circular plates, rectangular plates, spherical shells, and cylindrical shells. In the earlier work, we reported only equations for either asymptote of blast loading, i. e., the impulsive loading regime or the quasi-static loading regime.

This report extends and supplements the work of References 1 and 2. It includes revised analyses of plate response which achieve better agreement with experimental data from the literature, and new analyses for other structural elements which have been encountered in the design of suppressive structures. Some of the formulas apply for the simultaneous application of the two asymptotic loading conditions.

This work was performed for Edgewood Arsenal under Contract DAAA75-15-C-0083 as part of the suppressive structures program.

II. ANALYSIS

A. General

Most of the analyses which we have conducted in the suppressive structures program are based on energy solutions to estimate the ultimate load-carrying ability of structural components. The technique used to create these analyses was developed in References 1 and 2. A critical first step in this approach is to assume a final deformed shape of a structural element so the strain energy can be computed. In the impulsive loading realm, one then computes the kinetic energy imparted to the structure and equates this to the strain energy. In the quasi-static loading realm, one computes the work performed by the peak force deflecting the structure and equates this to the strain energy. References 1 and 2 used elementary rheological models, and data for beams and plates to illustrate the procedures. This report is a supplement on the response of plates and other structural elements. Earlier analyses for beams are still valid; however, plate solutions should be replaced with the following discussion, as additional data have led to modifications that give more accurate numerical results.

B. Clamped Circular Plates

The first plate solution will be for clamped circular plates subjected to either uniform impulse or uniform pressures. This solution adds additional terms to the strain energy expressions in References 1 and 2, as both bending and extensional action are present. An appropriate assumed deformed shape for a clamped deformed circular plate is

$$w = w_0 \left(1 - \frac{r}{R}\right) \quad (1)$$

The deformed shape is described by a polar coordinate system with its origin at the center of the plate. Because of symmetry, the deformed shape is independent of the angle θ and no shears exist. Equation (1) is an equation for a cone. It is an acceptable deformed shape, as at $r = 0$, the maximum deformation is finite ($w = w_0$), and at $r = R$, $w = 0$. The slope is not zero at $r = R$, as a plastically deforming plate is bent over the edge of the clamp along an abrupt yield line that has an angle change of $\Phi = 0 - (dw/dr)_r=R$, or $\Phi = (w_0/R)$.

Because no change in length occurs circumferentially at the boundary, there is no circumferential extensional strain; however, circumferential bending strain does occur. The circumferential plastic strain energy per unit differential length dr equals the plastic yield moment times the circumference times the circumferential curvature or $(\sigma_y h^2/4)$ times $(2\pi r)$ times $[(1/r)(dw/dr)]$. Radially, the deforming plate stores energy in membrane action. This radial strain energy per unit differential length dr equals the yield stress times the thickness times the circumference of a ring at location r , times the extensional strain. Using the well-known approximate extensional strain relationship $1/2(dw/dr)^2$ for the average change in radial strain means that the radial extensional strain energy stored in the plate per unit differential length dr is given by $(\sigma_y/2)$ times $(2\pi rh)$ times $(1/2)(dw/dr)^2$. The third and final amount of strain energy stored in a clamped plate is that associated with plastically bending the plate over the edge of the clamp. Bending strain energy along this yield line is calculated by multiplying the yield moment per unit width times the circumference of the plate times the change in angle at the edge of the plate or $(\sigma_y h^2/4)$ times $(2\pi R)$ times (w_0/R) . The total strain energy U is the sum of these contributions or

$$U = \underbrace{\left(\frac{\sigma_y h^2}{4}\right)(2\pi R)\left(\frac{w_0}{R}\right)}_{\text{bending over rim}} + \underbrace{\int_0^R (2\pi r) \left(\frac{\sigma_y h^2}{4}\right) \left(\frac{1}{r} \frac{dw}{dr}\right) dr}_{\text{circumferential bending}} + \underbrace{\int_0^R (\sigma_y/2)(2\pi rh) \left(\frac{1}{2}\right) \left(\frac{dw}{dr}\right)^2 dr}_{\text{radial extension}} \quad (2)$$

Differentiating Eq. (1), substituting it into Eq. (2), and gathering terms then yields

$$U = \frac{\pi}{2} \sigma_y h^2 w_0 + \frac{\pi}{2} \sigma_y h^2 w_0 \int_0^R \frac{dr}{R} + \pi \sigma_y h w_0^2 \int_0^R \frac{r dr}{R^2} \quad (3)$$

Or:

$$U = \pi \sigma_y h^2 w_0 + \frac{\pi}{2} \sigma_y h w_0^2 \quad (4)$$

The kinetic energy KE for a uniformly applied impulsive load imparted to a plate is obtained by summing the impulse squared divided by two times the incremental mass over the surface of the entire plate. This procedure leads to the following integration.

$$KE = \int_0^R \frac{I_r^2 (2\pi r)^2 (dr)^2}{2\rho h (2\pi r) (dr)} \quad (5)$$

Or:

$$KE = \frac{\pi I_r^2 R^2}{2\rho h} \quad (6)$$

Equating U [Eq. (4)] to KE [Eq. (6)] yields the asymptote for the impulsive loading realm.

$$\left[\frac{I_r R}{\sqrt{\rho \sigma_y} h^2} \right]^2 = 2 \left(\frac{w_0}{h} \right) + \left(\frac{w_0}{h} \right)^2 \quad \{ \text{circular plate, impulsive realm} \} \quad (7)$$

A comparison between Eq. (7) for a uniform impulse imparted to a clamped circular plate and experimental test data can be made using results by Florence.³ Residual permanent mid-span deformations were measured on clamped circular 6061-T6 aluminum plates and 1018-cold rolled steel plates that had been loaded uniformly with various thicknesses of sheet explosive. The 22 aluminum data points, 20 steel data points, and Eq. (7) are all shown in Figure 1. There is a reasonable agreement between Eq. (7) and the test results. If there exists a systematic error, it is a tendency for the analytical curve to slightly underestimate deformations whenever w_0/h is large. This error is probably caused by the assumed deformed shape not yielding the minimum strain energy. For small values of w_0/h , the analytical curve overestimates deformations. This error is probably created because we assume that deformations extend over the entire span of the plate. When loads and deformations are small the deformed shape undoubtedly covers only a portion of the entire plate.

A solution for a clamped circular plate in the quasi-static loading realm is obtained by computing the work and equating it to the strain energy. The work W_k is given by the integral of the maximum pressure times a differential area times the deflection of the differential area, and is expressed by Eq. (8).

$$W_k = \int_0^R P_w 2\pi r dr \quad (8)$$

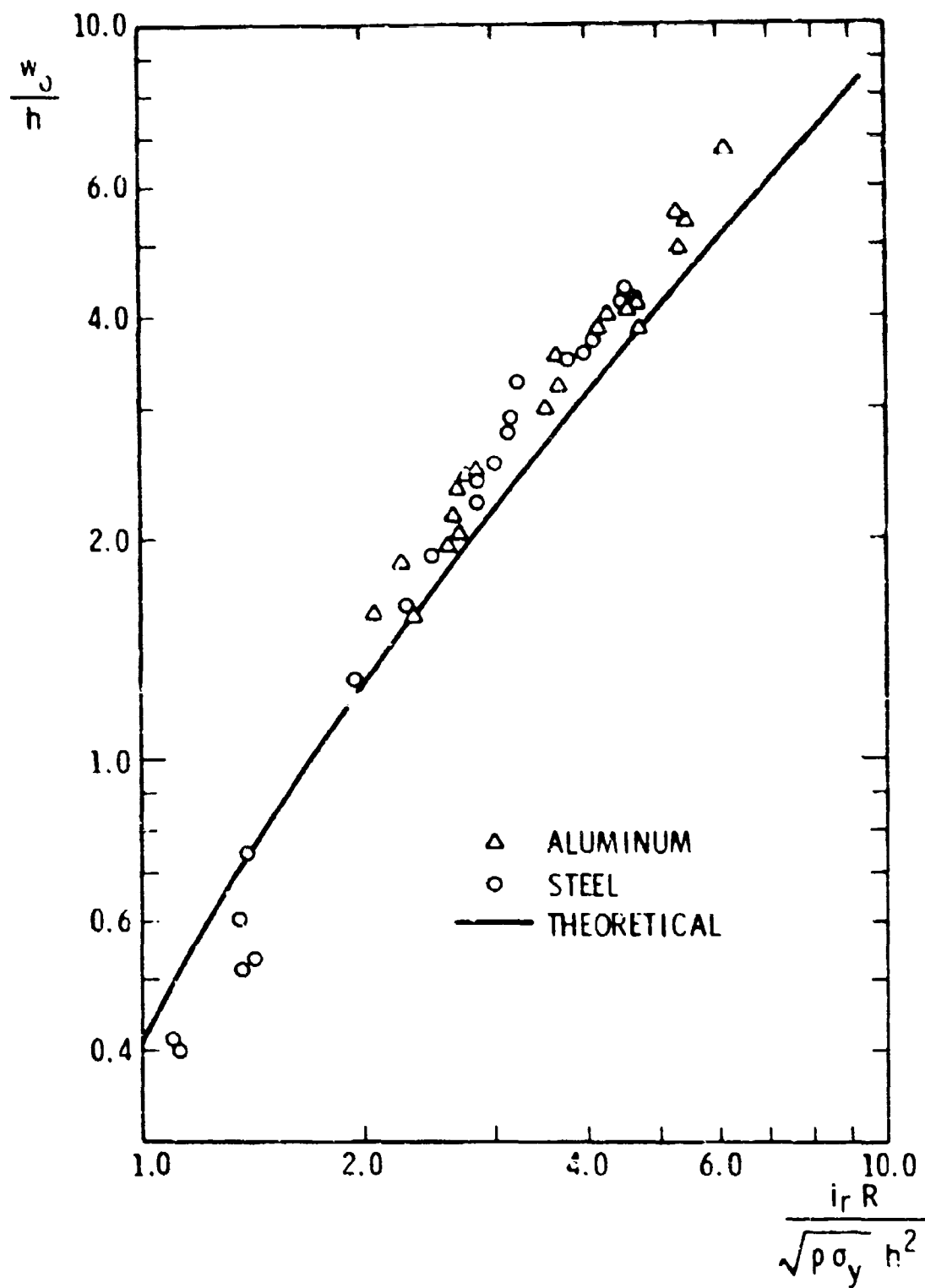


FIGURE 1. PLATE DEFORMATIONS IN AN IMPULSED CLAMPED CIRCULAR PLATE

Substituting the assumed deformed shape as given by Eq. (1) for w and factoring out constant terms then yields

$$WK = -\pi P w_o \int_0^R \left(r - \frac{r^2}{R} \right) dr \quad (9)$$

Or

$$WK = \frac{\pi}{3} P w_o R^2 \quad (10)$$

Equating U [Eq. (4)] to WK [Eq. (10)] yields the asymptote for the quasi-static loading realm

$$\left[\frac{PK^2}{w_o h^2} \right] = 3.0 + 1.5 \left[\frac{w_o}{h} \right] \quad \left\{ \text{circular plate quasi-static realm} \right\} \quad (11)$$

A comparison between Eq. (11) for a clamped circular plate with a uniform quasi-static pressure and experimental test data can be made using some test results by Ziliacus, Phyllact, and Shorlow.⁴ In these experiments, various thicknesses of steel plate were clamped over one end of a cylindrical explosive chamber. Various size pentolite charges were detonated at various locations inside the explosive chamber. This testing procedure means that short duration shocks are transmitted which eventually decay and cause a quasi-static pressure rise within the explosive chamber. By considering only those data where the impulsive energy imparted to the plates is small relative to the work performed by the quasi-static pressure rise, we are able to evaluate Eq. (11). This restriction means that we only used data for charges located at the far end of the explosive chamber.

Unfortunately, the quasi-static pressure rise for these tests had to be calculated for these NSRDC experiments. We used Figure B5 from Reference 1 to calculate p . Whenever p is calculated using Figure B5, it is an averaged pressure, and not a peak. Figure 2 shows a typical pressure history reported in Ref. 4. The first very intense peak is ignored entirely,* as it is the reflected shock wave which will be treated as an insignificant delta function. The quasi-static pressure rise as seen in Figure 2 is not smooth; many reverberations or reflected shocks can be seen. On the average, the peak quasi-static pressure is approximately 1.7 times a calculated smooth quasi-static pressure rise. Strain gage records in Reference 4 indicate that maximum plate response occurred well after the initial shock, but before significant decay of quasi-static pressure. Hence, the analytical line for this comparison will be given by 1.7 p , being substituted into Eq. (11), which gives Eq. (12).

*This procedure must be applied with caution because it is not generally true. It simply happens to apply for this particular set of experiments.

$$\begin{bmatrix} PK^2 \\ \sigma_1 h^2 \end{bmatrix} = 1.765 + 0.882 \begin{bmatrix} \dot{u}_0 \\ \dot{u}_1 \end{bmatrix} \quad (12)$$

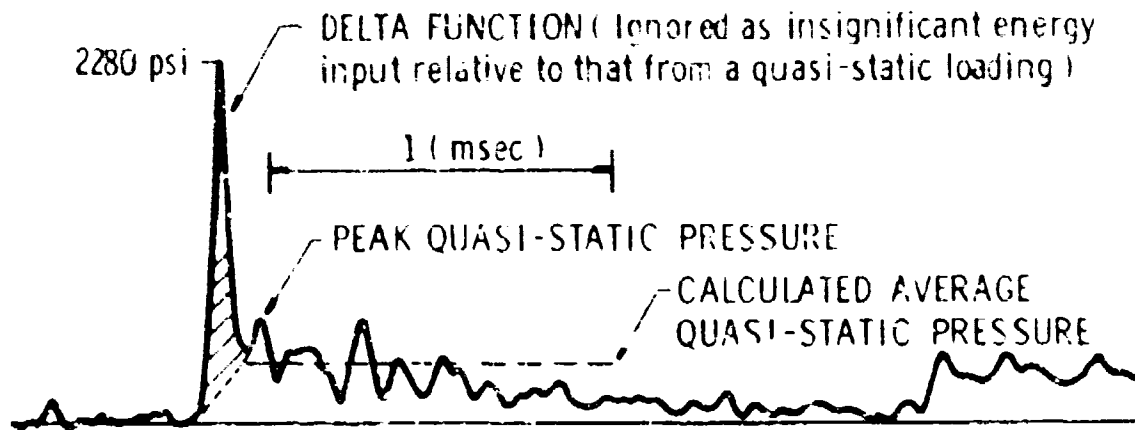


FIGURE 2. MEASURED LOADING IN NOKIA CIRCULAR PLATE TESTS

Plotted in Figure 3 are data points from Reference 4 and Eq. (12). Agreement is excellent over the entire range. Subsequent test results on square and rectangular plates, loaded pneumatically so no reverberations or reflected shocks are found, will show that no 1.7 factor is required for overshoot.

C. Clamped Rectangular Plates

The most general plate solution is for the plastic response of rectangular plates to either uniformly applied impulses or pressures. This solution introduces new complications because of extensional and bending shears. For a clamped rectangular plate, bending will occur along yield lines at the boundaries, and the plate will deform in membrane action. An appropriate deformed shape is assumed to be given by

$$w = w_0 \cos \frac{\pi x}{2A} \cos \frac{\pi y}{2B} \quad (13)$$

where

A and B are half spans

x and y are a rectangular coordinate system with origin at the center of the plate

This assumed deformed shape meets the appropriate deflection criteria in the middle and along the boundaries. The slope in the middle is zero, while the slope at the boundaries is the negative of the angle change when the plate is bent over the clamp. The strain energy

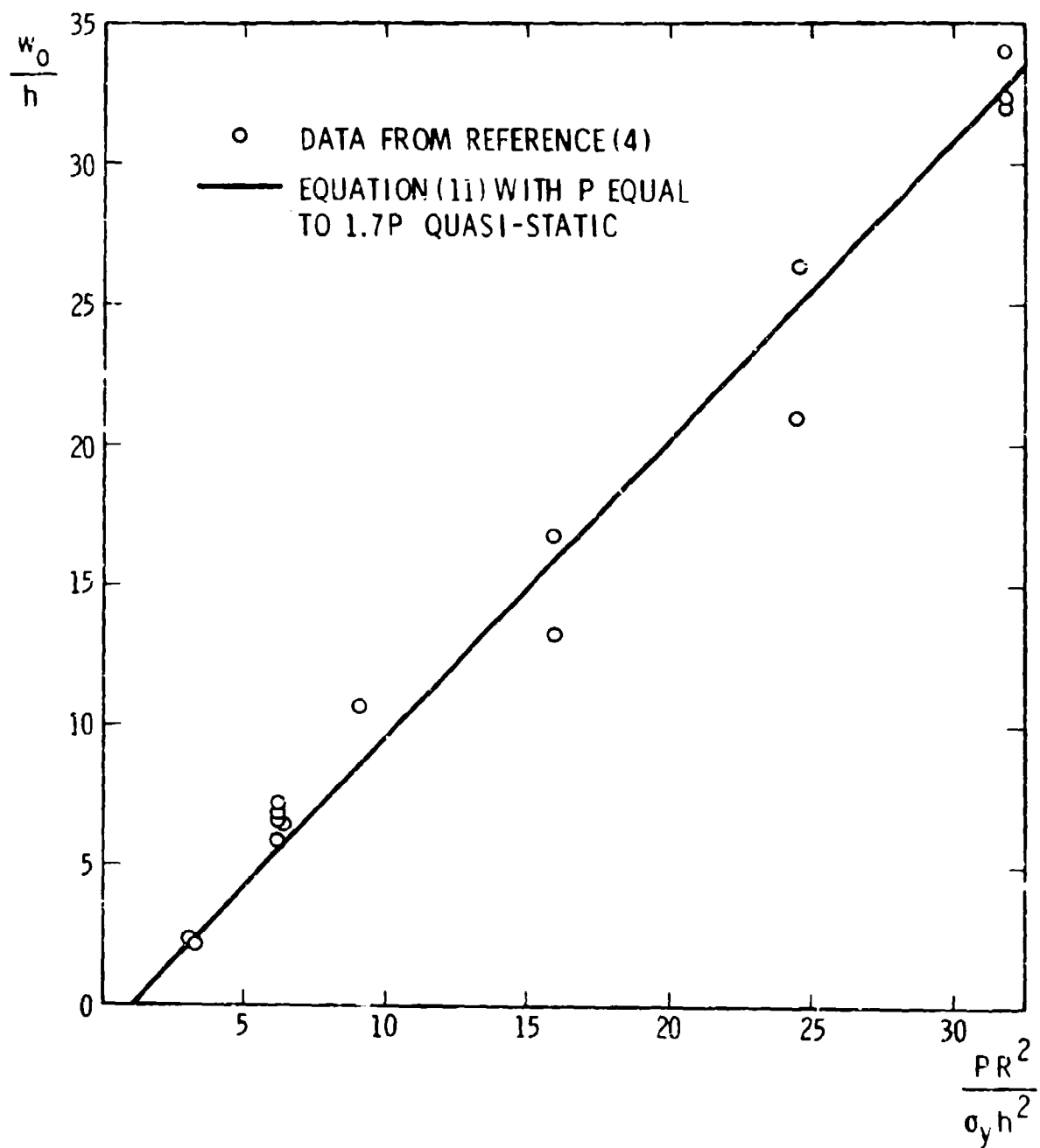


FIGURE 3. DEFORMATION IN QUASI-STATICALLY LOADED CIRCULAR PLATE

per unit volume in a structural element under a biaxial state of stress is:

$$\frac{U}{\text{Vol.}} = \int_{\text{strains}} [\sigma_{xx} d\epsilon_{xx} + 2\sigma_{xy} d\epsilon_{xy} + \sigma_{yy} d\epsilon_{yy}] \quad (14)$$

Because we have yielding, we will assume $\sigma_{xx} = \sigma_y$ and $\sigma_{yy} = \sigma_y$, but for the shearing stress we will use a Huber-Mises-Hencky distortion energy yield criteria of $\sigma_{xy} = (\sigma_y/\sqrt{3})$. At first glance, one would say that Mohr's circle for stress is a point if $\sigma_{xx} = \sigma_{yy}$; hence, no shears can occur. Such an observation is correct for any instant in time, but normal stress disturbances propagate faster than shearing disturbances. We are writing an energy expression for final state and do not care about the timing of events. It is sufficient for our purposes to know that plate distortions from normal stresses and from shearing stresses can occur at different times; thus, permitting the use of distortion energy principles to determine yield stresses. The normal extensional strains in a rectangular plate are similar to those in a circular plate with $\epsilon_{xx} = (1/2)(\partial w/\partial x)^2$ and $\epsilon_{yy} = (1/2)(\partial w/\partial y)^2$. The extensional shearing strain $\epsilon_{xy} = (\partial w/\partial x)(\partial w/\partial y)$ as a first approximation. These observations mean that the extensional strain energy U_e is given by:

$$U_e = 4 \int_0^X dx \int_0^Y dy \int_0^h dz \sigma_y \left[\frac{1}{2} \left(\frac{\partial w}{\partial x} \right)^2 + \frac{1}{2} \left(\frac{\partial w}{\partial y} \right)^2 \right] \\ + 4 \int_0^X dx \int_0^Y dy \int_0^h dz (2) \left(\frac{\sigma_y}{\sqrt{3}} \right) \left(\frac{\partial w}{\partial x} \right) \left(\frac{\partial w}{\partial y} \right) \quad (15)$$

Differentiating the deformed shape [Eq. (13)], substituting it into Eq. (15), and performing the required triple integration yields:

$$U_e = \frac{\pi^2}{8} \sigma_y h w_0^2 \left[Y^2 + X^2 \right] + \frac{4}{\sqrt{3}} \sigma_y h w_0^2 \quad (16)$$

Normal stresses associated with bending of the yield line along the clamp cause additional strain energy U_{bn} to be stored. This energy, analogous to similar terms for the circular plate, is given by:

$$U_{bn} = -4 \int_0^Y M_y \left(\frac{\partial w}{\partial x} \right)_{x=X} dy - 4 \int_0^X M_x \left(\frac{\partial w}{\partial y} \right)_{y=Y} dx \quad (17)$$

Substituting $(\sigma_y h^2)/4$ for M_y , differentiating the deformed shape so it can be evaluated at the boundary and further substituting then yields:

$$U_{bn} = 4 \left(\frac{\sigma_y h^2}{4} \right) \left(\frac{\pi w_o}{2Y} \right) \int_0^Y \cos \frac{\pi y}{2Y} dy + 4 \left(\frac{\sigma_y h^2}{4} \right) \left(\frac{\pi w_o}{2Y} \right) \int_0^X \cos \frac{\pi x}{2X} dx \quad (18)$$

Or:

$$U_{bn} = \sigma_y h^2 w_o \left[\frac{Y}{X} + \frac{X}{Y} \right] \quad (19)$$

Finally, there exists a shearing strain energy associated with bending U_{bs} in the localized zone around the yield lines. If the small deformation equation for shear strain, $\epsilon_{xy} = 2z \left(\partial^2 w / \partial x \partial y \right)$, is used, the energy U_{bs} per unit volume is given by:

$$\frac{U_{bs}}{\text{Vol.}} = 2 \left(\frac{\sigma_y}{\sqrt{3}} \right) \left(2z \frac{\partial^2 w}{\partial x \partial y} \right) \text{ at the boundaries} \quad (20)$$

If we assume that the localized shear zone is four plate thicknesses wide, Eq. (20) becomes

$$U_{bs} = \frac{4}{\sqrt{3}} \sigma_y (4) \int_0^{h/2} 2dz \int_0^Y dy (4h) (z) \left(\frac{\partial^2 w}{\partial x \partial y} \right)_{x=X} \\ + \frac{4}{\sqrt{3}} \sigma_y (4) \int_0^{h/2} 2dz \int_0^X dx (4h) (z) \left(\frac{\partial^2 w}{\partial x \partial y} \right)_{y=Y} \quad (21)$$

Or, after differentiating Eq. (13) to substitute for $\partial^2 w / \partial x \partial y$ at the boundary:

$$U_{bs} = \frac{32\pi^2}{\sqrt{3}} \frac{\sigma_y h w_o}{XY} \left[\int_0^{h/2} \int_0^Y \left[z \sin \frac{\pi y}{2Y} \right] dz dy + \int_0^{h/2} \int_0^X \left[z \sin \frac{\pi x}{2X} \right] dz dx \right] \quad (22)$$

Performing the required double integration then yields:

$$U_{bs} = \frac{16\pi}{\sqrt{3}} \sigma_y h^2 w_o \left[\frac{h}{X} + \frac{h}{Y} \right] \quad (23)$$

The total strain energy U stored in a rectangular plate is the sum of U_e plus U_{bn} plus U_{bs} or:

$$U = \frac{\pi^2}{8} \sigma_y h w_o^2 \left[\frac{Y}{X} + \frac{X}{Y} \right] + \frac{4}{\sqrt{3}} \sigma_y h w_o^2 + \sigma_y h^2 w_o \left[\frac{Y}{X} + \frac{X}{Y} \right] + \frac{16\pi}{\sqrt{3}} \sigma_y h^2 w_o \left[\frac{h}{X} + \frac{h}{Y} \right] \quad (24)$$

The kinetic energy KE imparted to a plate is not dependent upon the deformed shape. For a uniformly applied impulsive load imparted to a rectangular plate, the kinetic energy

is obtained by summing up the impulse squared divided by two times the incremental mass over the surface of the plate. The appropriate integration is given by:

$$KE = 4 \int_0^X \int_0^Y \frac{i_f^2 (dx)^2 (dy)^2}{2 \rho h (dx) (dy)} \quad (25)$$

or

$$KE = \frac{2 i_f^2 X Y}{\rho h} \quad (26)$$

Equating U [Eq. (24)] to KE [Eq. (26)] yields the asymptote for the impulsive loading realm.

$$\left[\frac{i_f^2 Y^2}{\rho \sigma_y h^4} \right] = \frac{1}{2} \left(\frac{w_o}{h} \right) \left[1 + \left(\frac{Y}{X} \right)^2 \right] + \frac{8\pi}{\sqrt{3}} \left(\frac{w_o}{h} \right) \left[\frac{h}{X} \right] \left[1 + \frac{Y}{X} \right] + \frac{\pi^2}{16} \left(\frac{w_o}{h} \right)^2 \left[1 + \left(\frac{Y}{X} \right)^2 \right] + \frac{2}{\sqrt{3}} \left(\frac{w_o}{h} \right)^2 \left(\frac{Y}{X} \right) \quad (27)$$

This is the general solution for an impulsively loaded plate. It can be compared to test data reported by Jones, et al.⁵ Rectangular plates with an aspect ratio Y/X equal to 1.695 were loaded with sheet explosive in these tests. Both hot-rolled mild steel plates and 6061-T6 aluminum plates were tested and can be seen plotted in Figure 4. Although various thicknesses of plate were used, we will use an average value for $(X/h)_{avg} = 10.2$ in the second term of Eq. (27). Using an average value for X/h creates very little error, as the $(w_o/h)^2$ membrane term predominates. Substituting for h/X in Eq. (27) yields Eq. (28), which is compared to the test data in Figure 4.

$$\left[\frac{i_f^2 Y^2}{\rho \sigma_y h^4} \right] = 5.76 \left(\frac{w_o}{h} \right) + 4.35 \left(\frac{w_o}{h} \right)^2 \quad (28)$$

Agreement is excellent when data are compared to Eq. (28) as in Figure 4. The little error which does occur for small values of w_o/h is probably caused by the deformed shape occupying only a portion of the full span when deformations are small.

A quasi-static loading realm solution for rectangular plates is developed if the work is equated to strain energy. The work Wk is given by Eq. (29) in a manner analogous to that for a circular plate.

$$Wk = \int_0^X \int_0^Y 4 Pw \, dx \, dy \quad (29)$$

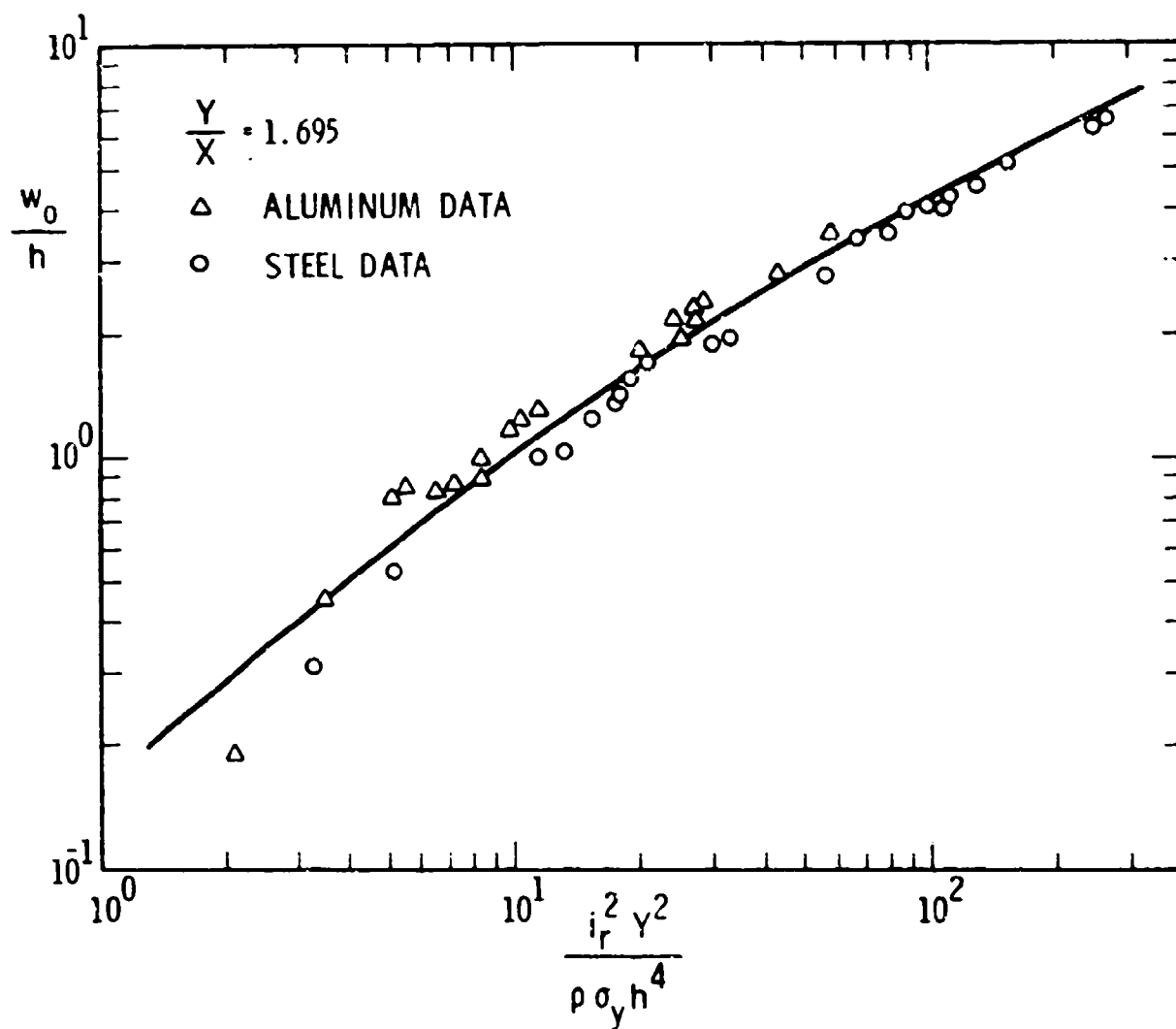


FIGURE 4. PREDICTED AND EXPERIMENTAL DEFORMATIONS IN UNIFORMLY IMPULSED RECTANGULAR PLATES

Substituting the assumed deformed shape as given by Eq. (13) and performing the required double integration then yields:

$$Wk = \frac{16}{\pi^2} P w_o X Y \quad (30)$$

Equating U [Eq. (24)] to Wk [Eq. (30)] yields the asymptote for the quasi-static loading realm.

$$\left[\frac{PX^2}{\sigma_y h^2} \right] = \frac{\pi^2}{16} \left[1 + \left(\frac{X}{Y} \right)^2 \right] + \frac{\pi^3}{\sqrt{3}} \left[\frac{h}{Y} \right] \left[1 + \frac{X}{Y} \right] + \frac{\pi^4}{128} \left(\frac{w_o}{h} \right) \left[1 + \left(\frac{X}{Y} \right)^2 \right] + \frac{\pi^2}{4\sqrt{3}} \left(\frac{w_o}{h} \right) \left[\frac{X}{Y} \right] \quad (31)$$

We can evaluate the validity of Eq. (31) by comparing it to test data taken by Hooke and Rawlings.⁶ In these experiments, clamped rectangular, mild-steel plates of various thicknesses and aspect (Y/X) ratios were subjected to step pneumatic pressures of very long duration. Because the pressures are pneumatically applied, no overshoot is present as in the quasi-statically, shock-loaded, circular plates. Figures 5 and 6 present some of these data in plots of scaled applied load [$PX^2/(\sigma_y h^2)$] as a function of scaled permanent mid-span deflection (w_o/h), for square plates and for rectangular plates with an (X/Y) of 1/2. An average value for scaled plate thickness (X/h) of 53.5 was used to determine the analytical lines in Figures 5 and 6. Because (X/h) varied over a limited range, and because its influence is only moderately important, a single value suffices when Eq. (31) is applied. Substituting for (X/Y) and (X/h) in Eq. (31) yields Eq. (32) for the square plate

$$\left[\frac{PX^2}{\sigma_y h^2} \right] = 1.95 + 2.96 \left(\frac{w_o}{h} \right) \quad \text{square plate test by Hooke} \quad (32)$$

and Eq. (33) for tests on a rectangular plate with X/Y equal to 1/2.

$$\left[\frac{PX^2}{\sigma_y h^2} \right] = 1.038 + 1.664 \left(\frac{w_o}{h} \right) \quad \text{rectangular plate tests by Hooke} \quad (33)$$

Agreement is excellent in Figures 5 and 6. Because test results are now consistent with the theoretical approach in both the impulsive and quasi-static loading realms, the physical viewpoints being reflected in this analysis appear to be substantiated, and we now feel we know how to handle structural members which are under a biaxial state of stress as well as a uniaxial one.

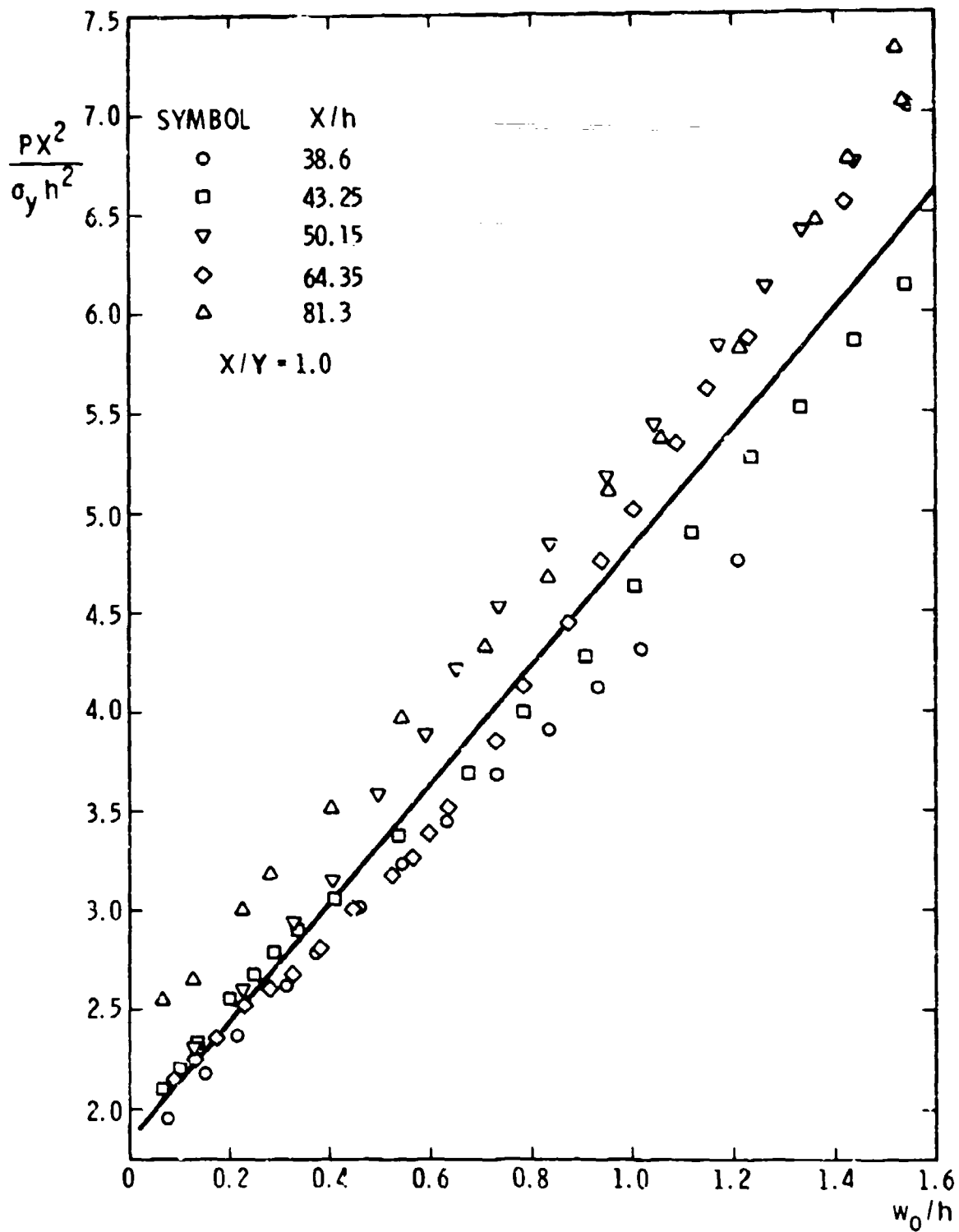


FIGURE 5 PERMANENT DEFORMATIONS IN QUASI-STATICALLY LOADED SQUARE PLATE

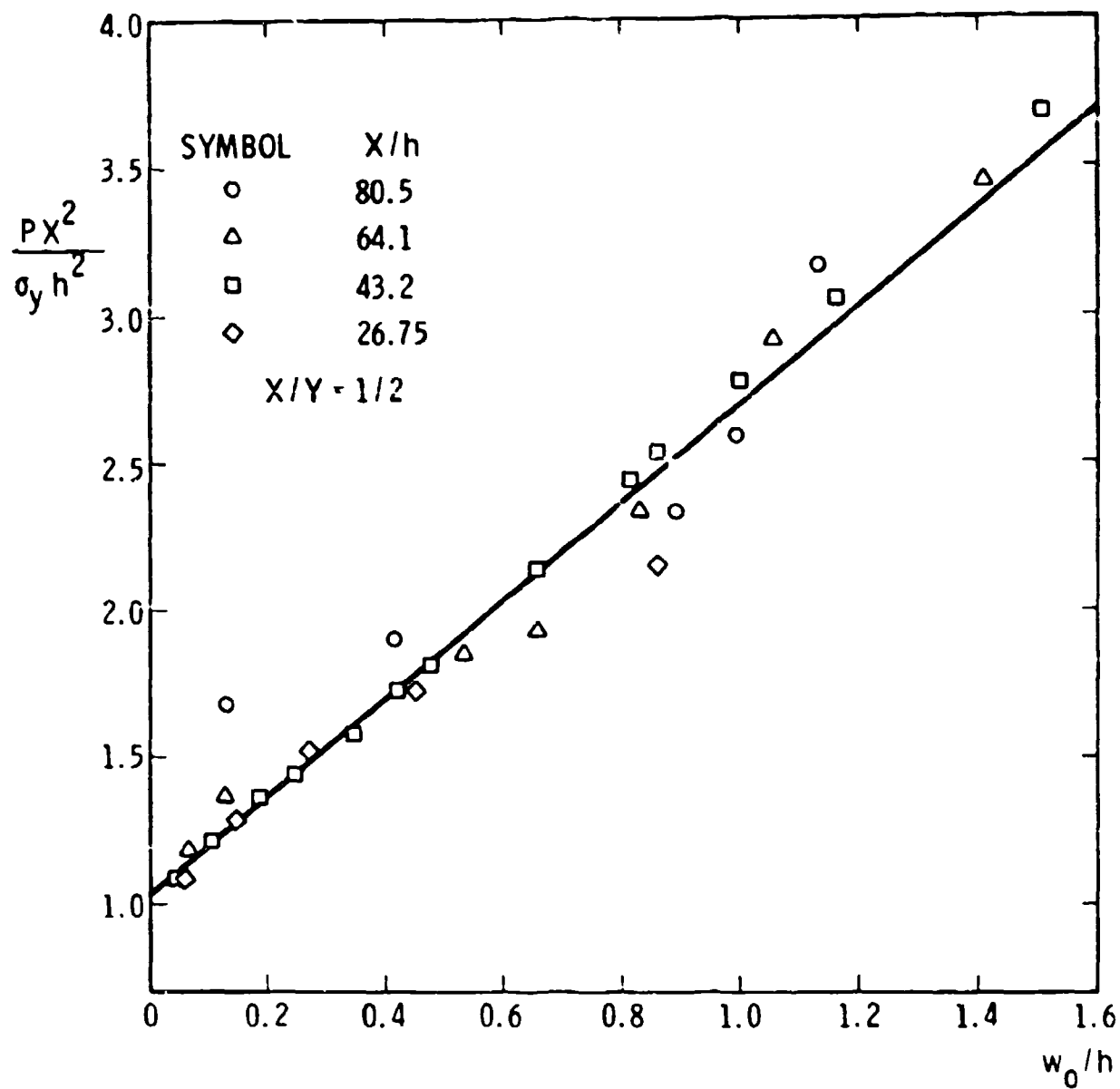


FIGURE 6. PERMANENT DEFORMATIONS IN QUASI-STATICALLY LOADED RECTANGULAR PLATE.

D. Rings Constraining I-beams

In the final design concept for the Category I structure, the basic structure consists of a series of interlocking vertical I-beams, supported by several rings or hoops. Because of this symmetry of the structure and the applied loading, ring response is represented by a uniform radial expansion. If the energy absorbed in deformation of the I-beams is neglected, then the ring response can be conveniently determined by an energy balance. To do this the kinetic energy imparted to the I-beams and rings by the initial blast wave, plus the work done by the quasi-static pressure as the cylinder expands, are equated to the strain energy in the rings. Figure 7 shows the geometry of the cylinder wall.

For uniform radial expansion the maximum possible kinetic energy imparted to the beams and ring is

$$KE = \int_{0}^{2\pi} \frac{1}{2} m \dot{r}^2 d\theta = \int_{0}^{2\pi} \frac{m}{2} \left(\frac{t_r L_B}{m} \right)^2 R_{Ri} d\theta = \frac{\pi R_{Ri} t_r^2 L_B^2}{m} \quad (35)$$

where m = mass per unit circumference

$$= A_R \rho \left(\frac{R_R}{R_i} \right) + \frac{L_B m_B}{CSB_{Ri}}$$

L_B -- length of the beams supported by one ring

m_B -- mass per unit length of the beams

CSB_{Ri} -- circumferential spacing of the beams as measured at R_{Ri}

R_R -- radius to the ring \bar{C}

A_R -- ring cross-sectional area

ρ -- density of the ring material

t_r -- reflected specific impulse

The maximum possible work done by the quasi-static pressure during the ring expansion is given by:

$$WK = \int_{0}^{2\pi} P L_B \cdot \Delta R \cdot d\theta = \int_{0}^{2\pi} P L_B \left(\frac{\Delta R}{R_R} \right) R_R d\theta = 2\pi R_R L_B \left(\frac{\Delta R}{R_R} \right) P \quad (36)$$

where

R -- mean radius of the interlocking I-beams

P -- peak quasi-static pressure

ΔR -- radial expansion of the ring

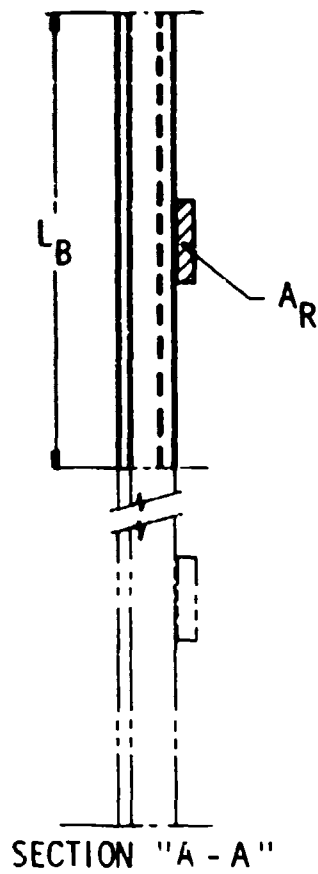
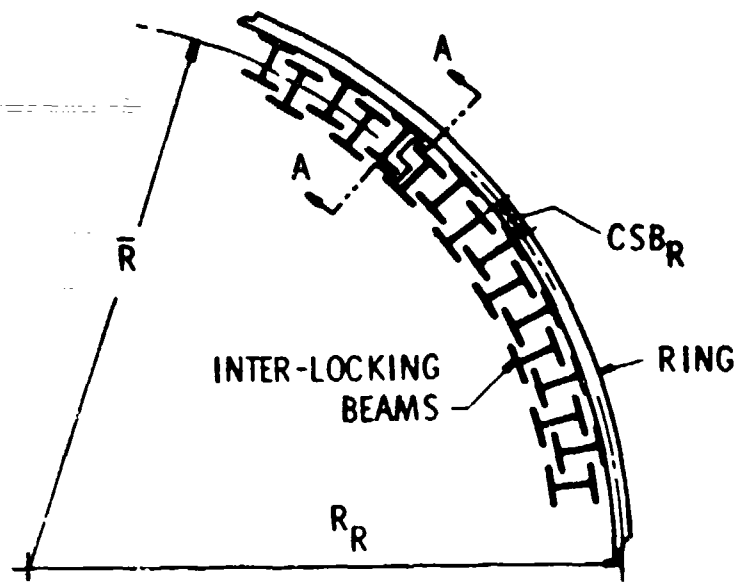


FIGURE 7. GEOMETRY OF BEAMS AND RINGS IN THE CYLINDER WALL

This expression assumes a constant quasi-static pressure and thus is conservative for rings with long response times. The degree of conservatism can be estimated from the response calculations reported in Reference 7. The calculated response time for a ring in the Category I prototype (with a cross-sectional area of 1.40 in²) is found from Reference 7 to be about 40 ms. Figure 8 shows the relationship between the response time of the ring and the decay of the quasi-static pressure. An estimate of the error is made by comparing the actual area under the pressure-time curve (impulse produced by the quasi-static pressure) to the area for constant P . The difference in areas, shown shaded, approximates the error. It is

$$\text{Error} = + \frac{\frac{P(40)}{2} - \frac{1}{2}(P + P_{40})(40)}{\frac{1}{2}(P + P_{40})(40)} \times 100 = +9.76\%$$

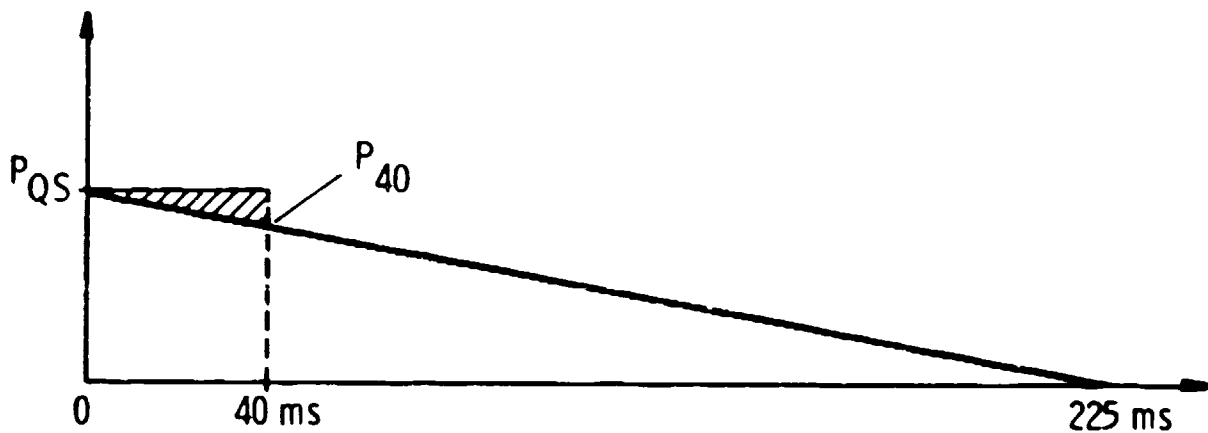


FIGURE 8. SCHEMATIC OF ERROR INCURRED BY ASSUMPTION OF CONSTANT QUASI-STATIC PRESSURE, P

For rigid-plastic behavior, the strain ϵ_r will equal $\Delta R/R_K$ and the strain energy in the ring undergoing radial expansion is given by:

$$U = A_R \int_0^{2\pi} \sigma_y \epsilon_r R_K d\theta = 2\pi R_K A_R \sigma_y \left(\frac{\Delta R}{R_K} \right) \quad (37)$$

where σ_y = yield stress of the ring material

Now, by equating

$$KE + Wk = U$$

the following relationship is obtained

$$\frac{i_p^2 L h}{m(A_R \sigma_y - R L_B P)} = 2 \left(\frac{\Delta R}{R_{Ri}} \right) \quad (38)$$

To estimate the degree of conservatism in Eq. (38) caused by neglecting the energy absorbed by plastic deformation of the I-beams, we again used the response calculations for the beams and rings described in Reference 7. Based on the calculated deformations for the beams and ring in the Category I prototype shield, the energy absorbed by each was computed for comparison. For the W8 X 67 beams supported by rings of cross-section 140 in², the plastic deflection of the inner beams between the center and lower rings was found to be about 1.6 inches which gives

$$w_o/L = 1.6/120 = 0.0133$$

An estimate of the strain energy absorbed by the beams with this center deflection is found from equation (C.21) of Reference 1

$$U = \frac{16 M_y w_o}{L} N \quad (39)$$

where

M_y - plastic moment of the beam $\approx 2.613 \times 10^6$ in-lb

N - number of beams in the inner layer = 157

Therefore the energy absorbed by the inner beams was

$$U = 16 (2.613 \times 10^6 \text{ in-lb}) (0.0133) (157) = 87.3 \times 10^6 \text{ in-lb}$$

If we conservatively assume that the outer layer of beams absorbs equal strain energy the total energy absorbed by the beams is

$$U = 2(87.3 \times 10^6 \text{ in-lb}) = 174.6 \times 10^6 \text{ in-lb}$$

The energy absorbed by the rings is estimated from the total radial deflection of the center ring from Reference 7 and Equation (37). From the table $\Delta R = 18.2$ in. so that

$$\frac{\Delta R}{R_R} = \frac{18.2}{283.5} = 0.0642$$

with

$$\begin{aligned} A_K &= 140 \text{ in}^2 \\ \sigma_t &= 40,000 \text{ psi} \end{aligned}$$

$$U = 2\pi R_K A_K \sigma_t \left(\frac{\Delta R}{R_K} \right) = 640.3 \times 10^3 \text{ in-lb}$$

Therefore the fraction of the total energy absorbed by the beams is

$$\eta = \frac{174.6 \times 100}{640.3 + 174.6} = 21.4$$

Although this number is high, because the assumption was made that the outer layer of beam absorbs the same amount of energy as the inner beams, it still indicates that there is a good deal of conservation in Eq. (38). Even so, the equation can be used to obtain quick, conservative estimates of the ring requirements.

E. Hemispheres (Domes)

If uniform loading is assumed on the inner surface of the sphere, and if the radial deflection at the base is assumed to be equal to that in the remainder of the hemisphere, then a uniform radial expansion exactly represents the dome response. This is shown in Figure 9. In actual structures the hemisphere usually will be secured at its base to a cylindrical section whose radial expansion may not match exactly that of the hemisphere. In other cases the

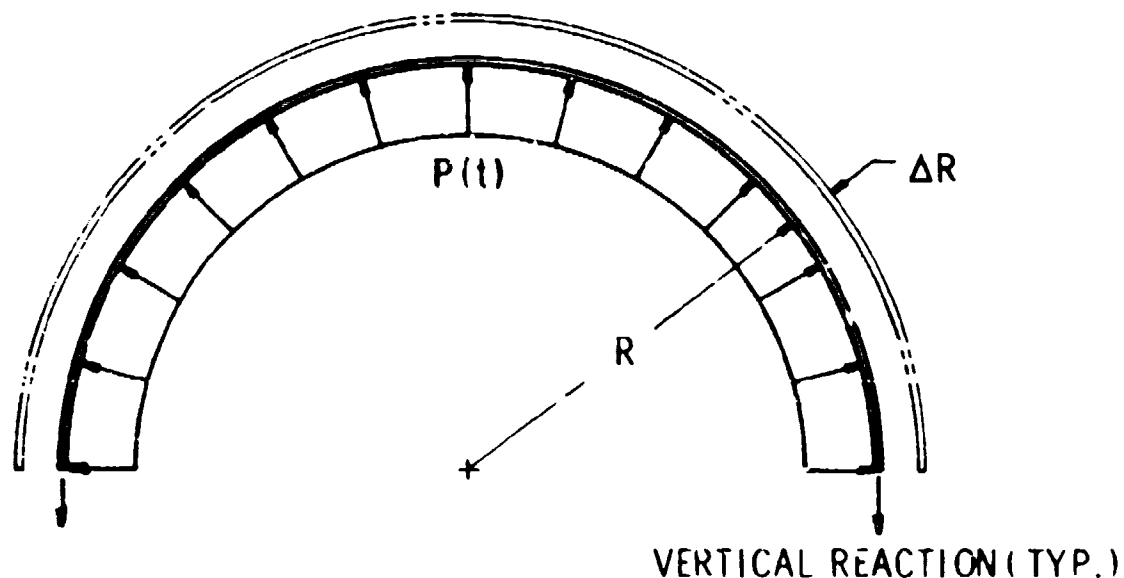


FIGURE 9. SYMMETRY OF DOME GEOMETRY, LOADING AND RESPONSE

dome may even be secured "rigidly" to a reinforced concrete foundation. The effect of this restraint on the total energy absorbed by the dome should be acceptably small for the "rigid" case and negligible for the other. The assumption of uniform loading is also acceptable, because the quasi-static pressure is uniform and the initial blast wave is approximately uniform depending on the charge location relative to the center of the hemisphere as well as the charge geometry. We have also observed that in the Category 1 design,⁷ the quasi-static pressure makes the greatest contribution to the dome thickness requirements.

As in the case of rings, the maximum dome deformation is obtained by equating the kinetic energy imparted to the dome by the initial blast wave, plus the work done by the quasi-static pressure during hemispherical dome expansion, to the strain energy absorbed by the dome. Kinetic energy is given by

$$KE = \int_A \frac{1}{2} m V^2 dA = \int_A \frac{u_r^2}{2m} dA = \frac{\pi R^2 u_r^2}{m} \quad (40)$$

where

- m mass per unit area of the dome
- R dome radius
- u_r specific reflected impulse

The work done by the quasi-static pressure during expansion of the dome is

$$WK = \int_A P \Delta R dA = 2\pi R^3 P \left(\frac{\Delta R}{R} \right) \quad (41)$$

P is the peak quasi-static pressure and its decay over the response time of the dome has been ignored.

Elastic strain energy per unit volume of the dome material is given by the well-known formula

$$dU = \frac{1}{2} (\sigma_x \epsilon_x + \sigma_y \epsilon_y + 2\sigma_{xy} \epsilon_{xy}) dxdydz \quad (42)$$

For rigid, perfectly-plastic behavior, shear stresses vanish and the stress is constant so that the strain energy doubles. Equation (42) can then be written

$$U = \int_A (\sigma_x \epsilon_x + \sigma_y \epsilon_y) h dA \quad (43)$$

where h = thickness of the material. Because the stresses and strains are uniform throughout the hemisphere for the assumption we have made, the equation further reduces to

$$U = h \int_A 2 \sigma \epsilon \, dA = 4 \pi R^2 h \sigma \epsilon \quad (44)$$

Since the strain can be expressed as

$$\epsilon = \frac{\Delta R}{R}$$

the strain energy finally becomes

$$U = 4 \pi R^2 h \sigma_y \left(\frac{\Delta R}{R} \right) \quad (45)$$

for a dome thickness h and yield stress σ_y .

Now, equating,

$$KE + Wk = U$$

The following relationship is obtained

$$\frac{i_f^2}{\rho h (2h\sigma_y - P R)} = 2 \left(\frac{\Delta R}{R} \right) \quad (46)$$

where ρh is replaced m in the kinetic energy term.

For some applications to suppressive shields, two concentric domes are used with a filler in between. The purpose of this arrangement is to defeat the fragments with the inner dome and filler, allowing the undamaged outer dome to resist the internal loads. This dome arrangement is given in Figure 10. Response of this dome arrangement differs from that of the single dome in the following ways.

- (1) The response is altered because of the added mass
- (2) The inner dome stretches along with the outer dome
- (3) The radial load is reduced because of the reduction in the loaded radius, but the total vertical load is unchanged because of the pressure acting on the ring which closes the bottom of the space between the domes.

Although the inner dome expands along with the outer dome and thus absorbs energy also, it is also possible that catastrophic rupture will initiate at fragment damage locations during

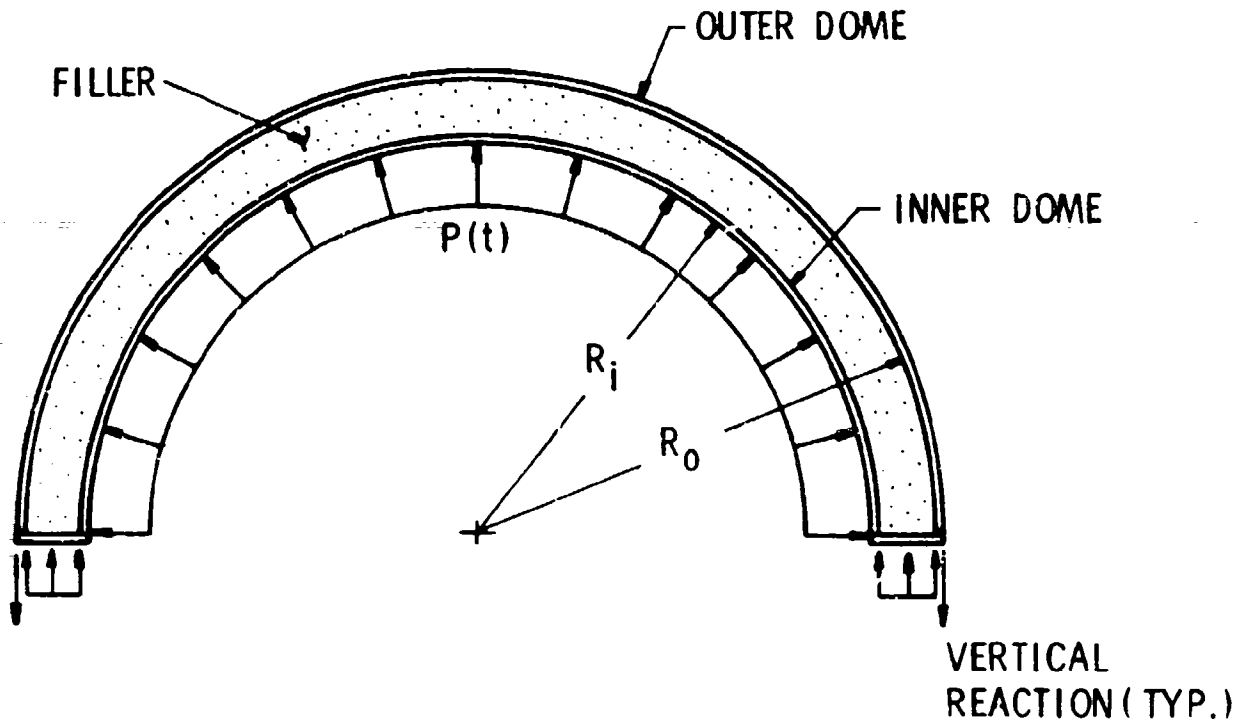


FIGURE 10. GEOMETRY OF THE DOUBLE-DOME SEPARATED BY FILLER MATERIAL

its expansion. Thus, the contribution of the inner dome to the strain energy is ignored. Also, the reduction in the loaded radius is ignored because the vertical loading is unchanged. Thus, a conservative estimate of the response is obtained by modifying only the mass in the kinetic energy term given by Eq. (40). Instead of $m = \rho h$ for a single dome we have

$$m = \rho h + m_a$$

where m_a = added mass produced by the inner dome and filler material divided by the area of the outer dome.

Equation (46) becomes simply

$$\frac{i_r^2}{(\rho h + m_a) (2 h \sigma_y - \bar{P} R)} = 2 \left(\frac{\Delta R}{R} \right) \quad (47)$$

for the double-dome arrangement. To date no comparisons with experiment have been made for either Eq. (46) or (47).

III. RESULTS

The results of the energy balance analyses presented here update and extend those given in References 1 and 2. Because these formulas now are rather numerous, we have summarized

them in an extensive table (Table 1), giving a description of the structural element, the assumed deformed shape, and the solution for combined impulsive and quasi-static blast loads. These formulas reduce to the quasi-static and impulsive loading asymptotes for $i_r = 0$ and $p = 0$, respectively. Symbols in Table 1 are defined in Table 2. No dimensions are given because the equations are in essentially dimensionless form, and correct for any self-consistent set of units.

IV. DISCUSSION

The energy solutions presented in this report should give designers additional tools for rapid estimation of plastic deformations in suppressive structures or elements of these structures, for the initial blast loading, for the longer duration quasi-static pressures and for both of these loads applied simultaneously. The revised equations for plate deformations consider strain energy terms not included in previous analyses, and also utilize deformed shapes which are closer to experimentally observed final deformations.

This report describes the current status of the work on a portion of the suppressive structures program. The energy solutions given here will undoubtedly be supplemented by other solutions or modified as more data on dynamic plastic responses in this program; notably BRL, NSWC White Oak, and Corps of Engineers at Huntsville, Alabama. Results on response prediction methods from these studies and other work in the literature should be compared as the program progresses. The energy methods are powerful and potentially quite useful because they yield relatively simple design formulas. They do, however, involve a number of simplifying assumptions and should not be expected to yield the accuracy in response prediction possible with a number of available dynamic response computer codes, nor can they predict time histories of deflections or strains. One should probably rely on the energy solutions for initial analysis and design, and to compare feasibility of different concepts. Then, designs can be refined by specific calculations using more complex and more nearly exact dynamic response computer programs. This was the procedure followed in the design of the Category 1 structure reported in Reference 7.

TABLE 1. SUMMARY OF ENERGY SOLUTIONS FOR ESTIMATING PLASTIC DEFORMATIONS ON BLAST-LOADED ELEMENTS

Structural Element	Deformed Shape	Response Formula for Combined Initial Impulse and Quasi-Static Pressure
Cantilever beam	$w = w_0 \left(1 + \cos \frac{\pi x}{2L} \right)$	$\frac{5.32 i_r^2 b^2 L}{\pi \rho A M_p (w_0/L)} = 2.16 - \frac{\rho b L^2}{M_p}$
Simply supported beam, bending only	$w = w_0 \left(1 + \frac{4x^2}{L^2} \right)$	$\frac{3 i_r^2 b^2 L}{4 \rho A M_p (w_0/L)} = 1.2 - \frac{\rho b L^2}{M_p}$
Clamped beam, bending only	$w = w_0 \cos \frac{\pi x}{L}$	$\frac{\pi i_r^2 b^2 L}{4 \rho A M_p (w_0/L)} = \pi^2 - \frac{\rho b L^2}{M_p}$
	$w = 2w_0 \left(1 + \frac{4x^2}{L^2} \right)$	$\frac{i_r^2 b^2 L}{\rho A M_p (w_0/L)} = 32 - \frac{\rho b L^2}{M_p}$
	$w = \frac{16w_0}{L^4} \left(x^2 - \frac{L^2}{4} \right)^2$	$\frac{15 i_r^2 b^2 L}{16 \rho A M_p (w_0/L)} = 23.99 - \frac{\rho b L^2}{M_p}$
	$w = Nw_0 \left(1 + \frac{4x^2}{L^2} \right)$	$\frac{i_r^2 b^2}{P_y \rho A} + \frac{4N^{4.15} \rho b L}{3P_y} \left(\frac{w_0}{L} \right) = \frac{16NM_y}{P_y L} \left(\frac{w_0}{L} \right)$
Beam bending, membrane and strain hardening $N = 1$, simply supported $N = 2$, clamped		$+ \frac{16}{3} \left(\frac{w_0}{L} \right)^2 + \frac{64E_y A}{5P_y} \left(\frac{w_0}{L} \right)^2$
Clamped Rectangular plate, bending, membrane and shear	$w = w_0 \cos \frac{\pi x}{2X} \cos \frac{\pi y}{2Y}$	$\frac{\pi^2 i_r^2 X^2}{8 \rho \sigma_y h^4 (w_0/h)} + \frac{\rho X^2}{\sigma_y h^2} = \frac{\pi^2}{16} \left[1 + \left(\frac{X}{Y} \right)^2 \right]$
		$+ \frac{\pi^2}{\sqrt{3}} \left(\frac{h}{Y} \right) \left[1 + \frac{X}{Y} \right] + \frac{\pi^4}{128} \left(\frac{w_0}{h} \right) \left[1 + \left(\frac{X}{Y} \right)^2 \right] + \frac{\pi^2}{4\sqrt{3}} \left(\frac{w_0}{h} \right) \left(\frac{X}{Y} \right)$

TABLE 1. SUMMARY OF ENERGY SOLUTIONS FOR ESTIMATING PLASTIC DEFORMATIONS OF BLAST-LOADED ELEMENTS (Cont'd)

Structural Element	Deformed Shape	Response Formula for Combined Initial Impulse and Quasi-Static Pressure
Clamped circular plate, bending and membrane action	$w = w_0 \left(1 - \frac{r}{R} \right)$	$\frac{3i_r^2 R^2}{2\rho\sigma_y h^2 (w_0/h)} + \frac{\rho R^2}{\sigma_y h^2} = 3 + \frac{3}{2} \left(\frac{w_0}{h} \right)$
Rings supporting I-beams	$\Delta R = \text{constant}$	$\frac{i_r^2 L_B^2}{2A_R \rho \sigma_y \left(1 + \frac{L_B M_B}{\rho A_R C S B_R} \right) \left(\frac{\Delta R}{R} \right)} = 1 - \frac{\rho R L_B B}{A_R \sigma_y}$
Hemisphere (dome)	$\Delta R = \text{constant}$	$\frac{i_r^2}{\rho} \left(\frac{\Delta R}{R} \right) = 1 - \frac{\rho R}{2\sigma_y h}$
Hemisphere with added mass, m_d	$\Delta R = \text{constant}$	$\frac{i_r^2}{\rho} \left(\frac{m_d}{\rho + \frac{m_d}{h}} \right) \left(\frac{\Delta R}{R} \right) = 1 - \frac{\rho R}{2\sigma_y h}$

TABLE 2. DEFINITION OF SYMBOLS USED IN TABLE 1

<u>Symbol</u>	<u>Definition</u>
A	beam cross-sectional area
A_R	ring cross-sectional area
b	loaded width of beam
CSB_R	circumferential beam spacing in the I-beam cylinder measured at R_R
h	thickness of plate or dome
i_r	specific reflected impulse from initial blast wave, plus reflections if applicable
L	length of beam for which the deformation is being determined
L_B	length of beam which is restrained by a single ring in the I-beam cylinder
m_a	mass per unit area of the inner dome and filler material for the double-dome roof
m_B	mass per unit length for the beams in the I-beam cylinder
M_p	beam plastic moment
N	factor in the beam equation; $N = 1$ for simple support, $N = 2$ for clamped support
P	quasi-static pressure
P_y	axial yield force of the beam
r	radius to arbitrary point on a circular plate
R	mean radius of the hemisphere (dome)
R_R	mean radius of the ring in the I-beam cylinder
ΔR	radial expansion of the ring or dome
w	lateral deflection of a beam or plate at point x or r , respectively
w_o	center deflection of a beam or plate
x	distance along the beam or plate, normally measured from the center
X	short semi-span of the plate
y	distance along plate center line normally measured from the plate center
Y	long semi-span of the plate
ρ	material density
σ_y	yield strength of the material

REFERENCES

1. W. E. Baker, P. S. Westine, P. A. Cox, and E. D. Esparza, Southwest Research Institute (San Antonio, Texas). Technical Report No. 1. Contract DAAD05-74-C J751. *Analysis and Preliminary Design of a Suppressive Structure for a Melt Loading Operation*, March 4, 1974.
2. P. S. Westine and W. E. Baker, Southwest Research Institute (San Antonio, Texas). Edgewood Arsenal Contractor Report EM-CR-76027, Report No. 6, Contract DAAA15-75-C-0083, *Energy Solutions for Predicting Deformations in Blast-Loaded Structures*, November 1975.
3. A. L. Florence, Circular Plate Under a Uniformly Distributed Impulse, *Journal of Solids and Structures*, 2, 37-47 (1966).
4. S. Ziliacus, W. E. Phyllaier, and P. K. Shorow, NSRDC, Bethesda, Maryland, Report No. 3987. *The Response of Clamped Circular Plates to Confined Explosive Loading*, February 1974, AD 782-518.
5. N. Jones, O. Uran, and S. A. Iekin, "The Dynamic Plastic Behavior of Fully Clamped Rectangular Plates," *Int. Jour. Solids Structures*, 6, 1499-1512 (1970).
6. R. Hooke and B. Rawlings, "An Experimental Investigation of the Behavior of Clamped, Rectangular, Mild Steel Plates Subjected to Uniform Transverse Pressure," *Inst. of Civil Engineers, Proceedings*, 42, 75-103 (1969).
7. W. E. Baker, P. A. Cox, E. D. Esparza, and P. S. Westine, Southwest Research Institute, (San Antonio, Texas). Edgewood Arsenal Contractor Report EM-CR-76031, Technical Report No. 9, Contract DAAA15-75-C-0083, *Design Study of a Melt Loading Operation*, November 1975.